Review of Scientific Instruments

Fast deuteron diagnostics using visible light spectra of ^{3}He produced by deuteron–deuteron reaction in deuterium plasmas

Cite as: Rev. Sci. Instrum. **92**, 053524 (2021); https://doi.org/10.1063/5.0034683
Submitted: 22 October 2020 • Accepted: 23 April 2021 • Published Online: 10 May 2021

K. Kimura, H. Matsuura, Y. Kawamoto, et al.

Review of Scientific Instruments ARTICLE scitation.org/journal/rsi

Fast deuteron diagnostics using visible light spectra of ^{3}He produced by deuteron–deuteron reaction in deuterium plasmas

Cite as: Rev. Sci. Instrum. 92, 053524 (2021); doi: 10.1063/5.0034683
Submitted: 22 October 2020 • Accepted: 23 April 2021 •
Published Online: 10 May 2021

K. Kimura,[1,a)] H. Matsuura,[1] Y. Kawamoto,[2] T. Oishi,[2,3] M. Goto,[2,3] K. Ogawa,[2,3] T. Nishitani,[4] M. Isobe,[2,3] and M. Osakabe[2,3]

AFFILIATIONS

[1] Department of Applied Quantum Physics and Nuclear Engineering, Kyushu University, 744 Motooka, Fukuoka 819-0395, Japan
[2] National Institute for Fusion Science, National Institutes of Natural Sciences, 322-6 Oroshi-cho, Toki 509-5292, Japan
[3] SOKENDAI (The Graduate University for Advanced Studies), 322-6 Oroshi-cho, Toki 509-5292, Japan
[4] Graduate School of Engineering, Nagoya University, Furo-cho, Chikusa-ku, Nagoya 464-8603, Japan

[a)] **Author to whom correspondence should be addressed:** k_kimura@nucl.kyushu-u.ac.jp

ABSTRACT

The fast deuteron (non-Maxwellian component) diagnostic method, which is based on the higher resolution optical spectroscopic measurement, has been developed as a powerful tool. Owing to a decrease in the D–H charge-exchange cross section, the diagnostic ability of conventional optical diagnostic methods should be improved for ~MeV energy deuterons. Because the ^{3}He–H charge-exchange cross section is much larger than that of D–H in the ~MeV energy range, the visible light (VIS) spectrum of ^{3}He produced by the dueteron–dueteron (DD) reaction may be a useful tool. Although the density of ^{3}He is small because it is produced via the DD reaction, improvement of the emissivity of the VIS spectrum of ^{3}He can be expected by using a high-energy beam. We evaluate the VIS spectrum of ^{3}He for the cases when a fast deuteron tail is formed and not formed in the ITER-like beam injected deuterium plasma. Even when the beam energy is in the MeV energy range, a large change appears in the half width at half maximum of the VIS spectrum. The emissivity of the VIS spectrum of ^{3}He and the emissivity of bremsstrahlung are compared, and the measurable VIS spectrum is obtained. It is shown that the VIS spectrum of ^{3}He is a useful tool for the MeV beam deuteron tail diagnostics.

I. INTRODUCTION

In a nuclear burning plasma, fast ions are always generated by fusion reactions, neutral beam injection (NBI), radiofrequency heating, and large-angle scattering.[1–4] Fast ions are essential for sustaining a nuclear burning plasma, and they collide with the particles in the plasma and provide them with energy; the plasma is heated through the repetition of this process. Fast ions may drive magnetohydrodynamic (MHD) instabilities such as sawteeth or toroidal Alfvén eigenmodes.[5–7] If the instability is driven, the confinement of fast ions deteriorates[7,8] and the efficiency of plasma heating by fast ions decreases. The elucidation of physics related to fast ions and MHD instabilities is one of the most important subjects in nuclear fusion research. These phenomena can be understood through the velocity distribution function of fast ions (fast ion tails). The slowing-down of fast ions appears as the shape of fast ion tails, and the gradient of fast ion tails affects MHD instabilities.[8,9] It is important to diagnose fast ion tails in experimental devices.

There are various types of fast ions, and we will focus on fast deuterons. The fast deuteron tail diagnostic method has been proposed or used in many experimental devices.[10] Among the fast deuteron tail measurement methods, collective Thomson scattering (CTS)[11] and fast ion D alpha (FIDA)[12] are direct measurements of the fast deuteron tail. CTS measurement contributed to the investigation of NBI-driven ion cyclotron instabilities.[13] FIDA has excellent energy resolution owing to the use of a visible light

(VIS) spectrometer. The deuteron is fully ionized in high temperature plasma and does not spontaneously emit photons. Therefore, the deuteron must be recombined by charge-exchange with an injected neutral particle beam. This method, which is known as charge-exchange recombination spectroscopy (CXRS), is a successful diagnostic approach.[14] FIDA uses a charge-exchange recombination reaction to measure the Balmer line of deuterons that are fully ionized in plasmas. In the ASDEX upgrade, during sawtooth crashes, fast deuteron redistribution was measured using FIDA.[15] To date, fast deuteron tail measurements have focused on fast deuteron tails that have been formed in the energy region of 10–100 keV. This energy range is suitable for the commonly used NBI injection energies. In an ITER-like experimental device with high-energy NBI, fast deuteron tails will be formed in the energy region on the order of MeV. In addition, alpha particles are produced by the DT reaction on the MeV range. In fusion reactors after the DEMO reactor, it is important to confirm the slowing-down and characteristics of loss of fast ions in the ITER because plasma heating occurs by fast ions with energy in the MeV region. When the energy of fast deuterons reaches the MeV region, even if the electron density is low, it becomes difficult for FIDA to obtain detailed information on fast deuteron tails.[10] This occurs because the charge-exchange reaction cross section between the hydrogenic ion and the hydrogenic atom sharply decreases in the MeV region. Higher energy fast deuterons are produced by the negative ion source tangential-injection NBI such as JT-60SA and ITER. These deuterons need to be charge-exchanged using this NBI. In addition, the measurement line of sight must be tangential because the fast deuteron is injected tangentially. Hence, the shift direction of beam emissions is the same as the shift direction of the FIDA spectrum, and the FIDA spectrum is contaminated by beam emissions.[16]

A measurement method, which uses a nuclear reaction during which the cross section rapidly increases at the high-energy region, is effective for the fast ion tail formed in the MeV region. In nuclear reactions that produce neutrons or gamma rays, the energy spectrum of nuclear reaction products contains information on the velocity distribution function of the reactants. Specifically, when the fast deuteron tail is formed in the velocity distribution function of the reactants, the energy spectrum of nuclear reaction products is distorted from the Gaussian component.[17] In JET, an attempt was made to estimate the fast ion tail formed by the third harmonic ion cyclotron resonance frequency heating by measuring the energy spectrum of neutrons.[18] In addition, a method using the anisotropy of neutron emissions for measuring small tail sizes has been proposed.[19] For gamma rays, Doppler broadening becomes wide in the wavelength (energy) spectrum.[20,21] This occurs because the wavelength (energy) spectrum of gamma rays is determined by the energy spectrum of the nuclide that emits gamma rays. The non-Gaussian component is the high-energy component in the energy spectrum of nuclides that emits gamma rays, and it is strongly affected by the Doppler effect. However, diagnostic methods using neutron and gamma rays have insufficient resolution of the detector to estimate the fast ion tail in detail. In the measurement conducted by Hellesen *et al.*, the energy resolution in the inferred fuel ion distribution function varied from 100 keV at low energies to 400 keV at the highest energies.[18] To measure the fast ion tail with high accuracy, it is desirable to use an instrument with higher energy resolution.

The energy (wavelength) resolution of a visible light (VIS) spectrometer is higher than that of instruments measuring neutrons and gamma rays. If the VIS spectrum of ^{3}He produced by the dueteron–dueteron (DD) reaction can be measured, a detailed diagnosis of fast deuteron tails may be possible. In the region where the relative energy is on the order of MeV, the charge-exchange cross section between $^3He^{2+}$ and H^0 is ~4 orders of magnitude larger than that between D^+ and H^0.[22] This characteristic is effective to perform fast deuteron tail diagnosis in the MeV range, which is difficult to do with FIDA. Furthermore, there is no contamination of the spectrum by beam emissions because elemental species is different from that of the beam. As a CXRS measurement for nuclear reaction products, there is a report that the velocity distribution function of thermalized alpha particles has been measured in TFTR DT plasmas.[23] In addition, the alpha particle measurement by CXRS using high-energy beams may be possible by calculation analysis in ITER DT plasmas.[24] This suggests that the VIS spectrum of ^{3}He may be measured. The energy of ^{3}He is smaller than the energy of alpha particles produced by the DT reaction. Therefore, the charge-exchange cross section of hydrogenic neutral particles and helium ions increases. In general, ^{3}He is not an ideal target for spectroscopic measurements owing to its low nuclear reaction rate. Possible solutions include an increase in ion temperature and the injection of a high-energy beam. These factors considerably increase the DD reaction rate and charge-exchange reaction rate. The effectiveness of using the ^{3}He VIS spectrum for fast deuteron diagnostics is assessed under the following two viewpoints. (1) The first viewpoint is the magnitude of the change in Doppler broadening of the VIS spectrum of ^{3}He with the fast deuteron tail formation. If the change in Doppler broadening of the VIS spectrum is small relative to the spectrometer resolution, it may not be possible to distinguish the change. Therefore, it is necessary to compare the amount of change in Doppler broadening in the VIS spectrum with and without the fast deuteron tail and the spectrometer resolution. (2) In spectroscopy, bremsstrahlung noise may obscure the VIS spectrum of ^{3}He. It is important to compare the emissivity of the VIS spectrum with the emissivity of bremsstrahlung.

The purpose of this paper is to examine whether the Doppler spread of the VIS spectrum of $^3He^+$ can be applied to diagnose fast deuteron tails. By limiting the calculation conditions at a high ion temperature and high beam energy, the VIS spectrum is evaluated when the beam deuteron tail is formed and not formed. The effectiveness of the proposed method is clarified on the basis of the above-mentioned two viewpoints and compared with FIDA.

II. ANALYSIS MODEL

We assumed a spatially uniform deuteron beam injected deuterium plasma. It was assumed that reactions (i.e., DD reaction and charge-exchange reaction) and photon emission occur isotropically. The steady-state deuteron velocity distribution function f_d was evaluated by solving the Fokker–Planck equation as follows:

$$\left(\frac{\partial f_d(v_d)}{\partial t}\right)^{\text{Coulomb}} + S(v_d) - \frac{f_d(v_d)}{\tau_p} = 0, \tag{1}$$

where v_d is the velocity of the deuteron and τ_p is the particle confinement time. The first term on the left-hand side of Eq. (1) is the Coulomb collision term. The second term is the source (deuteron

beam) term. The third term is the particle loss term. The source is assumed to be the isotropic deuteron beam, and the velocity distribution function of the deuteron is uniformly distributed. The $^3He^{2+}$ energy spectrum was evaluated by the following formula:[25]

$$\frac{dN_{^3He^{2+}}}{dE} = \frac{1}{2}\iint f_d(v_d) f_{d'}(v_{d'}) \sigma_{dd} \delta(E - E_{^3He^{2+}}) v_r dv_d dv_{d'}, \quad (2)$$

where

$$E_{^3He^{2+}} = \frac{1}{2} m_{^3He^{2+}} V_C^2 + \frac{m_n}{m_n + m_{^3He^{2+}}}(Q + E_r) + V_C \cos\theta_C \sqrt{\frac{2 m_n m_{^3He^{2+}}}{m_n + m_{^3He^{2+}}}(Q + E_r)}, \quad (3)$$

with $v_r = |\mathbf{v}_d - \mathbf{v}_{d'}|$. V_c is the center-of-mass velocity between deuterons. θ_c is the angle between the $^3He^{2+}$ velocity in the center-of-mass frame and the center-of-mass velocity. Q is the Q value of the DD reaction, and E_r represents the relative energy. The cross section of the DD reaction σ_{dd} was obtained from Bosch and Hale.[26] The energy spectrum of $^3He^{2+}$ recombined by the charge-exchange reaction was calculated as

$$\frac{dN_{^3He^+}}{dE_{^3He^+}} = \iint f_{^3He^{2+}}(v_{^3He^{2+}}) f_{H^0}(v_{H^0}) \sigma_{CX} \times \delta(E_{^3He^+} - E_{^3He^{2+}}) v_r dv_{^3He^{2+}} dv_{H^0}, \quad (4)$$

where H^0 denotes the neutral light hydrogen and σ_{CX} is the charge-exchange reaction cross section of H^0 and $^3He^{2+}$. The $^3He^{2+}$ velocity distribution function $f_{^3He^{2+}}$ was evaluated using Eq. (1). The neutral light hydrogen distribution f_{H^0} has monoenergy distribution. The neutral light hydrogen density n_{H^0} was calculated by the following equation: $n_{H^0} = P_{H^0}/(E_{H^0} \times A \times v_{H^0})$, where A is the cross section of the diagnostic beam for charge-exchange. Of note, the diagnostic (charge-exchange) beam is separate from the heating beam. We assumed that the ^3He velocity vector does not change before and after the charge-exchange reaction. The charge-exchange cross section was obtained from the National Institute for Fusion Science database.[22] The expected photon spectrum of $^3He^+$ was evaluated as

$$\frac{dN_{ph}}{d\lambda} = \int \frac{dN_{^3He^+}}{dE_{^3He^+}} \delta(E - E_{photon}) dE_{^3He^+} \frac{dE}{d\lambda}, \quad (5)$$

where

$$E_{photon} = E_{photon0}\left(\frac{\sqrt{1 - (v_{^3He^+}/c)^2}}{1 - (v_{^3He^+}/c)\cos\theta}\right). \quad (6)$$

In Eq. (6), $E_{photon0}$ is the transition energy and c is the speed of light. θ represents the angle between the observation line of sight and the $^3He^+$ velocity vector. The expected VIS spectrum is expressed by the quantity per unit solid angle. The upper-level principal quantum number ($n = 4$) has four types of subshells (e.g., s, p, d, and f); the transition from 4s has large charge-exchange cross section and large branching ratio. Therefore, in this study, we considered only the 3p–4s transition. The effect of the halo can be neglected in the beam energy range of this paper. The spectrum of bremsstrahlung was evaluated as

$$\frac{dN_{brem}}{d\lambda} = \frac{1.9 \times 10^{-36} n_e n_d Z_{eff} \bar{g}_{ff}}{T_e^{1/2} \lambda^2 E_{brem}} \exp\left(-\frac{hc}{T_e \lambda}\right), \quad (7)$$

with $E_{brem} = hc/\lambda$. Z_{eff} is the effective charge, $\bar{g}_{ff}$ is the temperature-averaged Gaunt factor, and h is the Planck constant. In this analysis, we assumed that $Z_{eff} = 1.6$ and $\bar{g}_{ff} = 5$. The diagnostic ability $\xi \times \zeta$ was defined as

$$\xi \times \zeta = \frac{\int \frac{dN_{tail}}{d\lambda} - \frac{dN_{Maxwellian}}{d\lambda} d\lambda}{\int \frac{dN_{Maxwellian}}{d\lambda} d\lambda} \times \frac{\left(\frac{dN_{tail}}{d\lambda} - \frac{dN_{Maxwellian}}{d\lambda}\right)_{peak}}{\left(\frac{dN_{brem}}{d\lambda}\right)_{peak}}, \quad (8)$$

where the tail indicates the case of beam tail formation and Maxwellian is the case of no tail formation. This equation is expressed as the product of the skewness of the VIS spectrum in the case of beam tail formation with respect to the case of no tail formation (ξ) and the emissivity ratio for bremsstrahlung (ζ). The signal-to-noise ratio (SNR) was defined as

$$\frac{S}{N} = \frac{\int S d\lambda}{\frac{1}{\eta}\sqrt{(\int S d\lambda + \int C d\lambda)\eta}}, \quad (9)$$

where S is the fast ^3He signal and C is the bremsstrahlung signal. The effective optical throughput of the spectrometer η was defined as $\varepsilon t_{exp} QET$. ε is the etendue, t_{exp} is the exposure time, QE is the quantum efficiency, and T is the optical transmission. We assumed that $\varepsilon = 5\ mm^2$ sr, $t_{exp} = 5$ s, $QE = 90\%$, $T = 15\%$, and the wavelength range is 0.1 nm. Table I shows the parameters used in the analysis. V represents the plasma volume. E_{NBI} is the neutral beam energy. P_{NBI} is the neutral beam power.

TABLE I. Calculation parameters.

Parameter	Value
E_{NBI} (deuterium) (MeV)	0.3–1.5
P_{NBI} (deuterium) (MW)	16.5, 33
E_{H^0} (hydrogen) (MeV)	1.0
P_{H^0} (hydrogen) (MW)	16.5
A (m^2)	0.1
T_e (keV)	20
T_d (keV)	20
n_e, n_d (m^{-3})	2.0×10^{19}
τ_p (s)	3
V (m^3)	800

III. RESULTS AND DISCUSSION

Figure 1 shows the deuteron velocity distribution functions for different beam energies. Change in the beam energy alters the size of the beam tail. This occurs because the density of deuterons injected by NBI is inversely proportional to the beam energy. In addition, the size of the bulk component depends on the beam energy. This occurs because the calculations were made in such a way as to conserve the density of deuterons. Therefore, with an increase in the beam tail

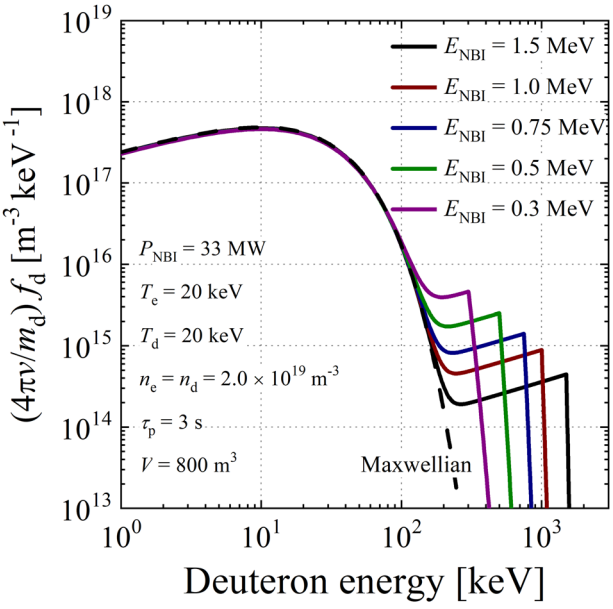

FIG. 1. Deuteron velocity distribution functions when P_{NBI} = 33 MW, T_e = T_d = 20 keV, and n_e = n_d = 2.0 × 10^{19} m^{-3} for several beam-injection energies in a beam injected ITER-like plasma.

size, the size of the bulk component will be reduced in the opposite direction.

Figure 2 shows the $^3He^{2+}$ energy spectra for different beam energies. If the deuteron velocity distribution function is Maxwellian, the $^3He^{2+}$ energy spectrum will be close to the Gaussian distribution (shown as a dashed line). When the beam tail is formed, the maximum value of the $^3He^{2+}$ energy spectrum increases. This occurs because the cross section of the DD reaction increases at a high relative energy so that the emission rate of $^3He^{2+}$ increases. When the beam energy increases, the distortion of the $^3He^{2+}$ energy spectrum from the Gaussian distribution becomes large because the $^3He^{2+}$ energy increases.

Figure 3 shows the $^3He^+$ VIS spectrum (expected) for different (a) beam energies and (b) beam powers. This graph is drawn as a semi-log graph. The emissivity of the VIS spectrum is ~1% compared to the emissivity of bremsstrahlung. This ratio is comparable to the CXS measurement for slowing-down alpha particles

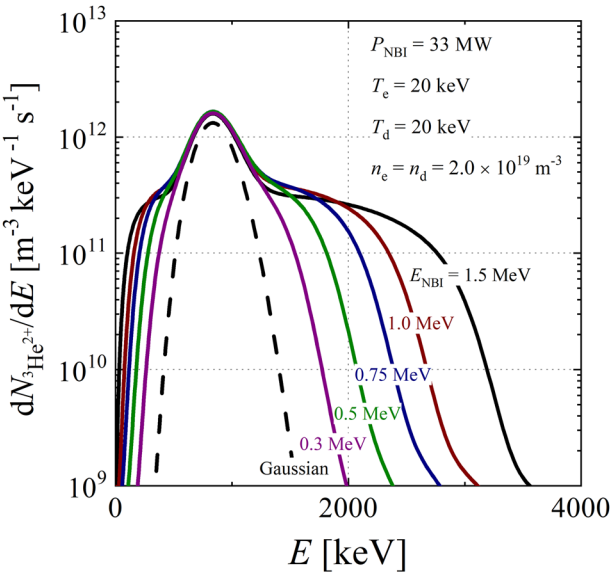

FIG. 2. Energy spectra of $^3He^{2+}$ produced by the DD reaction when P_{NBI} = 33 MW, T_e = T_d = 20 keV, and n_e = n_d = 2.0 × 10^{19} m^{-3} for several beam-injection energies.

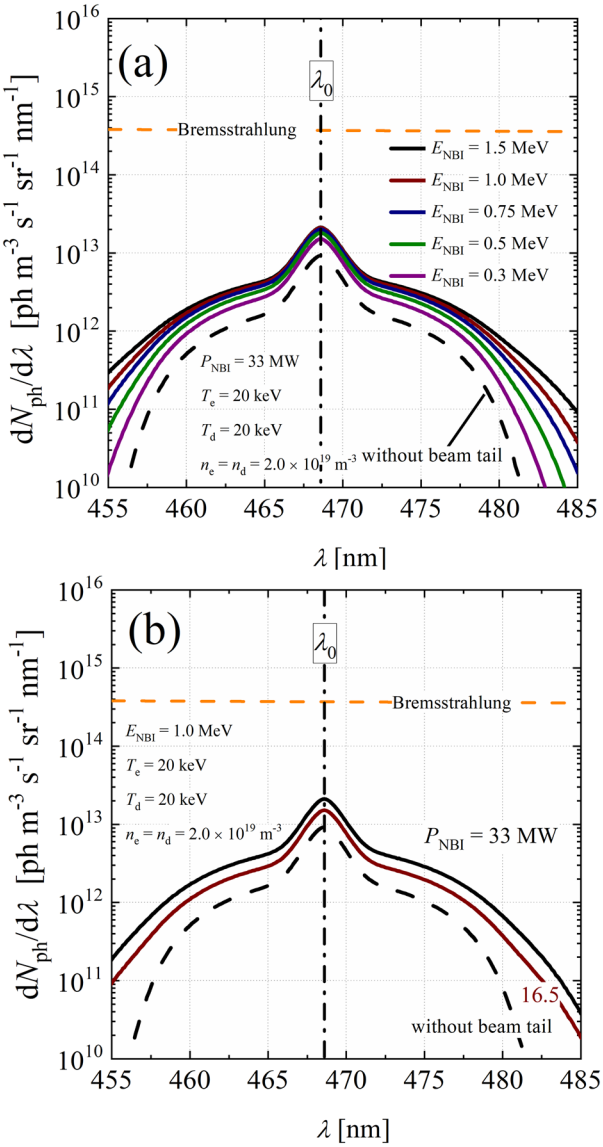

FIG. 3. VIS spectra (solid line) of $^3He^+$ when T_e = T_d = 20 keV and n_e = n_d = 2.0 × 10^{19} m^{-3} along with the bremsstrahlung spectrum (broken line): (a) E_{NBI} dependences and (b) P_{NBI} dependences.

TABLE II. S/N ratios for several beam energies when P_{NBI} = 33 MW, T_e = T_d = 20 keV, and n_e = n_d = 2.0 × 10^{19} m^{-3}.

E_{NBI} (deuterium) (MeV)	S/N ratio at (472 ± 0.05 nm)	S/N ratio at (477 ± 0.05 nm)
1.5	25	11
1.0	24	10
0.75	22	9.5
0.5	20	7.8
0.3	16	6.0

in TFTR.[23] Thus, the spectrum in the range of λ_0–478 nm may be measured using long-time exposure. The emissivity of the VIS spectrum is dependent on the beam energy. This occurs because, when the beam power is fixed, the size of the beam tail is inversely proportional to the beam energy. The emissivity is also dependent on the beam power. This can be explained by the fact that the DD reaction rate changes when the beam energy is fixed and the beam power is changed. If the $^3He^+$ VIS spectrum is measured beyond 478 nm, we can obtain more detailed information about the beam tail.

The SNR was evaluated for (a) in Fig. 3. The results are summarized in Table II. In the beam energy range of 0.5–1.5 MeV, the SNR is large and accurate measurements can be expected. Even though the intensity of the bremsstrahlung is two orders of magnitude greater than the intensity of the signal, the SNR is greater than 1 because noise is defined as the uncertainty of the bremsstrahlung (i.e., the square root of the intensity of the bremsstrahlung) in this paper. The SNR was evaluated when the beam energy was fixed at 1 MeV and the plasma temperature was varied. In the plasma temperature range of 18–20 keV, the SNR is large and accurate measurements can be expected (Table III). The electron density cannot be higher than 2 × 10^{19} m^{-3} because it would increase the intensity of the bremsstrahlung and reduce the size of the fast deuteron tail. NBI with beam energies above 0.5 MeV will be installed in the experimental device after JT-60SA. It will be the experimental device after ITER that can maintain the high plasma temperature for a long time. Therefore, it is difficult to apply the proposed method to the present-day experimental device.

We estimated the halo density relative to the NB density. When the beam energy is 1 MeV, the halo density is on the order of 10^9 m^{-3}. The NB density is on the order of 10^{13} m^{-3}, which is four orders of magnitude higher than halo density. When the beam energy is 0.3 MeV, the halo density is on the order of 10^{12} m^{-3}. The NB density is on the order of 10^{14} m^{-3}, which is two orders of magnitude higher than halo density. In addition, the D(H)–^{3}He charge-exchange cross section is smaller than that of the beam H^0 because the energy of the bulk D^0 is about a few keV. Therefore, the effect of the halo can be neglected in the beam energy range of this paper.

TABLE III. S/N ratios for several plasma temperatures when E_{NBI} = 1.0 MeV, P_{NBI} = 33 MW, and n_e = n_d = 2.0 × 10^{19} m^{-3}.

Temperature (keV)	S/N ratio at (472 ± 0.05 nm)	S/N ratio at (477 ± 0.05 nm)
20	24	10
18	18.5	8.0
15	12	5.1

Figure 4 shows the normalized $^3He^+$ VIS spectrum (expected) for different (a) beam energies and (b) beam powers. The value at λ = 472 nm (thermalized ^{3}He influence becomes sufficiently small) in the $^3He^+$ VIS spectrum was used for normalization. This graph is drawn as a linear graph. With an increase in the beam energy, the half width at half maximum (HWHM) of the VIS spectrum

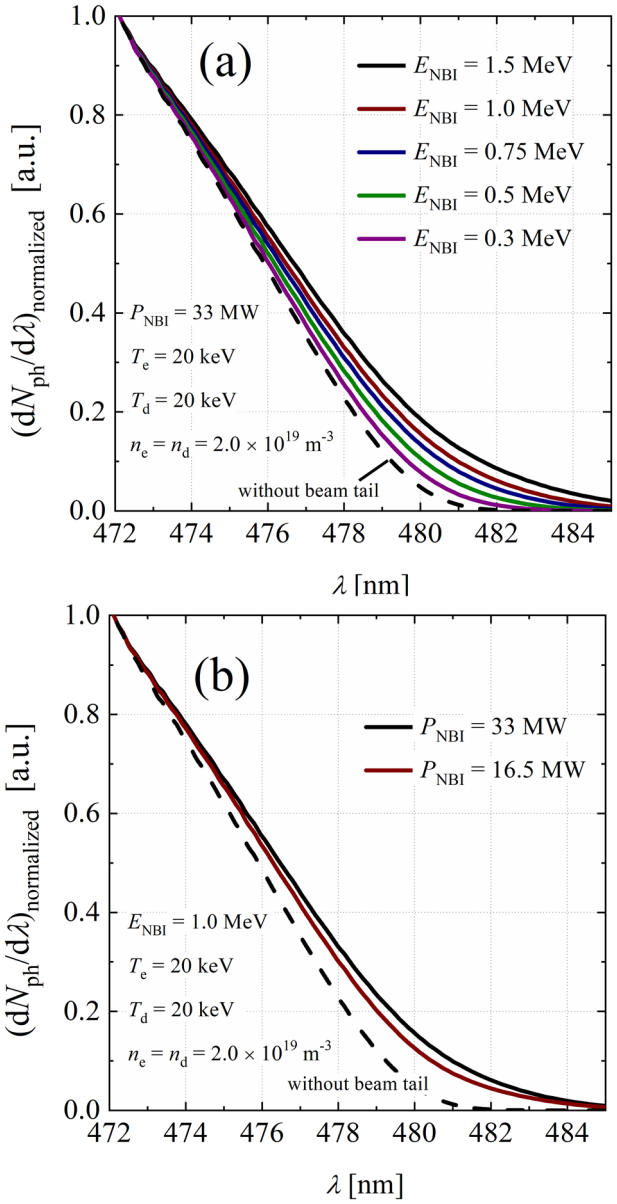

FIG. 4. VIS spectra of $^3He^+$ normalized by the value at λ = 472 nm when T_e = T_d = 20 keV and n_e = n_d = 2.0 × 10^{19} m^{-3}: (a) E_{NBI} dependences and (b) P_{NBI} dependences.

increased. This occurred owing to the high proportion of $^3He^+$ with the energy greater than 0.8 MeV when the beam energy is high. When the beam power increases, the HWHM increases, which is similar to the case of increasing beam energy. By defining $\Delta\lambda_{HWHM}$ as the difference in HWHM when the beam tail is formed and when it is not, $\Delta\lambda_{HWHM}$ is ~0.6 nm under the conditions of E_{NBI} = 1.0 MeV and P_{NBI} = 33 MW. In the VIS range, the resolution of the spectrometer of ITER is ~20 pm,[24] which is sufficient for detecting $\Delta\lambda_{HWHM}$ in the VIS spectrum. Thus, it is possible to distinguish between the case where the beam tail is formed and the case where the beam tail is not formed in the VIS spectrum. The change in plasma temperature and the change in beam energy can be distinguished by simultaneously looking at the HWHM and the emissivity of the VIS spectrum. When the temperature is changed, both the HWHM and the emissivity change. In this case, the emissivity changes more than that when the beam energy is changed. Therefore, even if the change in HWHM is the same, distinction can be made based on the change in emissivity. In the case of beam power, the distinction can be made from the reaction rate of the DD reaction rather than the emissivity of the VIS spectrum. When the beam power is fixed and the beam energy is varied, the reaction rate of the DD reaction is almost unchanged. On the contrary, when the beam energy is fixed and the beam power is varied, the reaction rate of the DD reaction changes significantly. Therefore, even if the change in HWHM is the same, distinction can be made based on the change in the reaction rate of the DD reaction.

Figure 5 shows the beam energy dependence of $\Delta\lambda_{HWHM}$ in the VIS spectra. An increase in the beam energy and beam power gains $\Delta\lambda_{HWHM}$. The energy resolution of the proposed method in the primary deuteron distribution function can be estimated from Fig. 5. To keep the SNR high, the wavelength is assumed to be divided every 0.1 nm. At a beam energy of around 1 MeV, the resolution for the beam energy is estimated to be ~150 keV. The gradient of $\Delta\lambda_{HWHM}$ as a function of beam energy depends on the beam power. Therefore, the energy resolution in the velocity distribution function improves with increasing beam power. Even if the entire $^3He^+$ VIS spectrum cannot be measured, the shape of the beam tail can be estimated from the relationship between $\Delta\lambda_{HWHM}$ and emissivity.

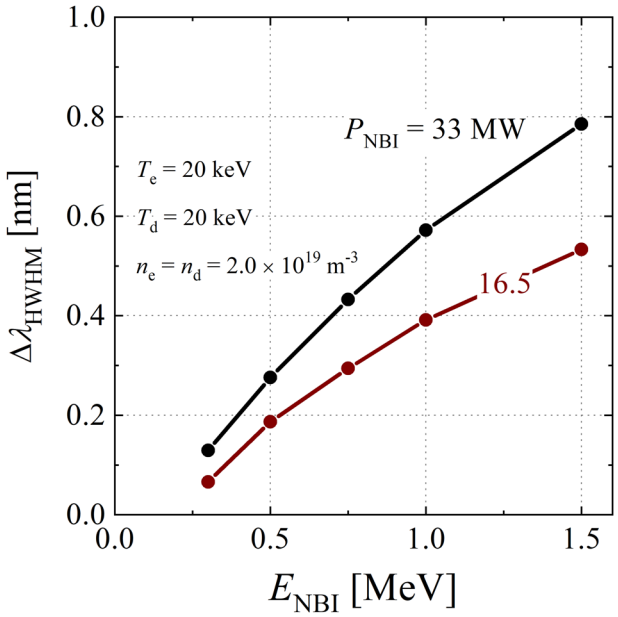

FIG. 5. $\Delta\lambda_{HWHM}$ (difference in HWHM when the beam tail is formed and when it is not formed) as a function of E_{NBI} for several beam powers when $T_e = T_d$ = 20 keV and $n_e = n_d = 2.0 \times 10^{19}$ m^{-3}.

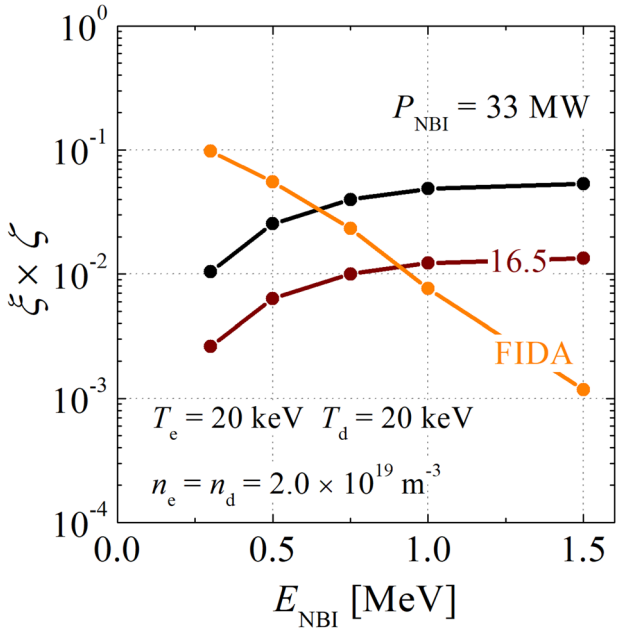

FIG. 6. MeV range ion tail diagnostic ability $\xi \times \zeta$ (products of the skewness of the VIS spectrum and the emissivity ratio for bremsstrahlung) of the ^3He VIS spectrum (black and red lines) as a function of E_{NBI} along with that of FIDA (orange line) for $T_e = T_d$ = 20 keV and $n_e = n_d = 2.0 \times 10^{19}$ m^{-3}.

Figure 6 shows the beam energy dependence of diagnostic ability for FIDA and VIS spectrum of ^3He. In the case of FIDA, the beam power of the deuterium beam was 33 MW. The beam energy of the diagnostic beam was assumed to be 100 keV to avoid the influence of contamination of the spectrum due to beam emissions. The diagnostic beam power was 3.6 MW. When P_{NBI} is 33 MW in the VIS spectrum of ^3He, it was comparable to FIDA's diagnostic ability for a beam tail of E_{NBI} = 0.75 MeV. Comparing the diagnostic ability of FIDA with that of ^3He VIS spectra, it is determined that ^3He is more sensitive than FIDA when the beam energy is on the order of MeV. This occurs owing to the large difference between D–H and ^3He–H charge-exchange cross sections when the relative energy reaches the MeV order.

Throughout the simulations, we assumed a uniform plasma. The temperatures, densities, and deuterium beam (energetic deuteron) in the actual plasma have spatial distributions. To select the line of sight of the spectrometer, it is necessary to perform simulations by considering spatial distributions.

IV. CONCLUSION

This paper shows a possibility of Doppler broadening of the VIS spectra of energetic ^{3}He produced by the DD reaction to diagnose the deuteron beam tail in the deuteron velocity distribution function. The VIS spectra of ^{3}He for the cases when a beam tail is formed and not formed in deuterium beam injected deuterium plasmas were evaluated under conditions when a large amount of ^{3}He is generated by the DD reaction increasing ion temperature and injecting high-energy beam. The change in Doppler broadening of the VIS spectrum of ^{3}He is sufficiently larger compared to the resolution of the current spectrometer, and a detailed observation of the size and shape of the beam tail can be expected. The emissivity of the VIS spectrum is ~1% compared to the emissivity of bremsstrahlung. The VIS spectrum may be measured using long-time exposure. The VIS spectrum of ^{3}He is a useful tool for the beam ion tail diagnostics in low density and high ion temperature operation. In the future, the evaluation will be performed by assuming an actual experimental device. If the observability increases, the beam tail shape will be measured by the experiment.

DATA AVAILABILITY

The data that support the findings of this study are available from the corresponding author upon reasonable request.

REFERENCES

[1]B. C. Stratton, R. V. Budny, H. H. Duong, D. K. Mansfield, S. S. Medley, M. H. Redi, R. J. Fonck, G. R. McKee, A. Ödblom, F. Wising, R. K. Fisher, J. M. McChesney, P. B. Parks, M. P. Petrov, and N. N. Gorelenkov, Rev. Sci. Instrum. **68**, 269 (1997).
[2]J. G. Cordey and M. J. Houghton, Nucl. Fusion **13**, 215 (1973).
[3]T. H. Stix, Nucl. Fusion **15**, 737 (1975).
[4]H. Matsuura, S. Sugiyama, K. Kimura, S. Kajimoto, T. Nishitani, K. Ogawa, Y. Kawamoto, M. Isobe, and M. Osakabe, Nucl. Fusion **60**, 066007 (2020).
[5]T. C. Hender, J. C. Wesley, J. Bialek, A. Bondeson, A. H. Boozer, R. J. Buttery, A. Garofalo, T. P. Goodman, R. S. Granetz, Y. Gribov, O. Gruber, M. Gryaznevich, G. Giruzzi, S. Günter, N. Hayashi, P. Helander, C. C. Hegna, D. F. Howell, D. A. Humphreys, G. T. A. Huysmans, A. W. Hyatt, A. Isayama, S. C. Jardin, Y. Kawano, A. Kellman, C. Kessel, H. R. Koslowski, R. J. La Haye, E. Lazzaro, Y. Q. Liu, V. Lukash, J. Manickam, S. Medvedev, V. Mertens, S. V. Mirnov, Y. Nakamura, G. Navratil, M. Okabayashi, T. Ozeki, R. Paccagnella, G. Pautasso, F. Porcelli, V. D. Pustovitov, V. Riccardo, M. Sato, O. Sauter, M. J. Schaffer, M. Shimada, P. Sonato, E. J. Strait, M. Sugihara, M. Takechi, A. D. Turnbull, E. Westerhof, D. G. Whyte, R. Yoshino, H. Zohm, and the ITPA MHD, Disruption and Magnetic Control Topical Group, Nucl. Fusion **47**, S128 (2007).
[6]R. J. Hastie, Astrophys. Space Sci. **256**, 177 (1997).
[7]A. Fasoli, C. Gormenzano, H. L. Berk, B. Breizman, S. Briguglio, D. S. Darrow, N. Gorelenkov, W. W. Heidbrink, A. Jaun, S. V. Konovalov, R. Nazikian, J.-M. Noterdaeme, S. Sharapov, K. Shinohara, D. Testa, K. Tobita, Y. Todo, G. Vlad, and F. Zonca, Nucl. Fusion **47**, S264 (2007).
[8]N. N. Gorelenkov, S. D. Pinches, and K. Toi, Nucl. Fusion **54**, 125001 (2014).
[9]S. E. Sharapov, B. Alper, H. L. Berk, D. N. Borba, B. N. Breizman, C. D. Challis, I. G. J. Classen, E. M. Edlund, J. Eriksson, A. Fasoli, E. D. Fredrickson, G. Y. Fu, M. Garcia-Munoz, T. Gassner, K. Ghantous, V. Goloborodko, N. N. Gorelenkov, M. P. Gryaznevich, S. Hacquin, W. W. Heidbrink, C. Hellesen, V. G. Kiptily, G. J. Kramer, P. Lauber, M. K. Lilley, M. Lisak, F. Nabais, R. Nazikian, R. Nyqvist, M. Osakabe, C. Perez von Thun, S. D. Pinches, M. Podesta, M. Porkolab, K. Shinohara, K. Schoepf, Y. Todo, K. Toi, M. A. Van Zeeland, I. Voitsekhovich, R. B. White, V. Yavorskij, ITPA EP TG, and JET-EFDA Contributors, Nucl. Fusion **53**, 104022 (2013).
[10]D. Moseev, M. Salewski, M. Garcia-Muñoz, B. Geiger, and M. Nocente, Rev. Mod. Plasma Phys. **2**, 7 (2018).
[11]H. Bindslev, J. A. Hoekzema, J. Egedal, J. A. Fessey, T. P. Hughes, and J. S. Machuzak, Phys. Rev. Lett. **83**, 3206 (1999).
[12]W. W. Heidbrink, K. H. Burrell, Y. Luo, N. A. Pablant, and E. Ruskov, Plasma Phys. Controlled Fusion **46**, 1855 (2004).
[13]A. G. Shalashov, E. V. Suvorov, L. V. Lubyako, H. Maassberg, and the W7-AS Team, Plasma Phys. Controlled Fusion **45**, 395 (2003).
[14]R. J. Fonck, D. S. Darrow, and K. P. Jaehnig, Phys. Rev. A **29**, 3288 (1984).
[15]B. Geiger, M. Weiland, A. S. Jacobsen, D. Rittich, R. Dux, R. Fischer, C. Hopf, M. Maraschek, R. M. McDermott, S. K. Nielsen, T. Odstrcil, M. Reich, F. Ryter, M. Salewski, P. A. Schneider, G. Tardini, and The ASDEX Upgrade Team, Nucl. Fusion **55**, 083001 (2015).
[16]C. M. Muscatello, W. W. Heidbrink, R. L. Boivin, C. Chrystal, C. S. Collins, Y. Fujiwara, and H. Yamaguchi, Rev. Sci. Instrum. **90**, 073504 (2019).
[17]L. Ballabio, G. Gorini, and J. Källne, Phys. Rev. E **55**, 3358 (1997).
[18]C. Hellesen, M. Gatu Johnson, E. Andersson Sundén, S. Conroy, G. Ericsson, J. Eriksson, H. Sjöstrand, M. Weiszflog, T. Johnson, G. Gorini, M. Nocente, M. Tardocchi, V. G. Kiptily, S. D. Pinches, S. E. Sharapov, and JET EFDA Contributors, Nucl. Fusion **53**, 113009 (2013).
[19]S. Sugiyama, H. Matsuura, and D. Uchiyama, Phys. Plasmas **24**, 092517 (2017).
[20]M. Nocente, M. Tardocchi, V. G. Kiptily, P. Blanchard, I. Chugunov, S. Conroy, T. Edlington, A. M. Fernandes, G. Ericsson, M. Gatu Johnson, D. Gin, G. Grosso, C. Hellesen, K. Kneupner, E. Lerche, A. Murari, A. Neto, R. C. Pereira, E. Perelli Cippo, S. Sharapov, A. Shevelev, J. Sousa, D. B. Syme, D. Van Eester, G. Gorini, and JET-EFDA Contributors, Nucl. Fusion **52**, 063009 (2012).
[21]Y. Kawamoto and H. Matsuura, Fusion Eng. Des. **144**, 62 (2019).
[22]See https://dbshino.nifs.ac.jp for Data from NIFS DATABASE.
[23]G. McKee, R. Fonck, B. Stratton, R. Bell, R. Budny, C. Bush, B. Grek, D. Johnson, H. Park, A. Ramsey, E. Synakowski, and G. Taylor, Phys. Rev. Lett. **75**, 649 (1995).
[24]A. Kappatou, E. Delabie, R. J. E. Jaspers, and M. G. von Hellermann, Nucl. Fusion **52**, 043007 (2012).
[25]H. Brysk, Plasma Phys. **15**, 611 (1973).
[26]H.-S. Bosch and G. M. Hale, Nucl. Fusion **32**, 611 (1992).